

SEVENTH EUROPEAN ROTORCRAFT AND POWERED LIFT AIRCRAFT FORUM

Paper No. 73

**AEROSPATIALE
SURVEY OF WIND TUNNEL TESTING
OF SMALL AND LARGE SCALE ROTORS**

J.P. SILVANI & A. VUILLET

Bureau Etudes - Société Nationale Industrielle Aérospatiale

Helicopter Division

Marignane, France

September 8 - 11, 1981

**Garmisch-Partenkirchen
Federal Republic of Germany**

**DEUTSCHE GESELLSCHAFT FUER LUFT- UND RAUMFAHRT e.V.
GOETHESTR. 10, D-5000 KOELN 51, F.R.G.**

AEROSPATIALE SURVEY OF WIND TUNNEL TESTING OF SMALL AND LARGE SCALE ROTORS*

J.P. SILVANI & A. VUILLET

Bureau d'Etudes - Société Nationale Industrielle Aérospatiale

Helicopter Division

Marignane, France

INTRODUCTION

In order to study the detailed aerodynamic and dynamic behaviour of the isolated rotor, Aerospatiale, partially sponsored by the French Ministry of Defense (DRET and STPA/HE), has supported for many years extensive wind tunnel tests on Mach scaled rotors.

The scale of the rotor mock-ups varies from roughly one tenth in the Chalais-Meudon wind tunnel to one third in Modane. In this latter case, the hub is fitted with a swash-plate, general and cyclic inputs : both include the capability for a wide range of shaft angle settings.

A description of the ONERA test facilities is developed as well as wind tunnel rotor technology, stress and strain, pressure, Laser velocity measurements and visualizations. The effect of tip shapes, twist and profile distribution on performance and vibration is discussed. Special emphasis is placed on the influence of the OA family airfoils as measured in Modane and of rotor blade tip shapes measured in Chalais.

Furthermore, rotor icing tests, performance at very high speed in autorotation and tilt rotor tests are presented.

GENERAL DESCRIPTION

The general performance obtained by Aerospatiale when using ONERA's wind-tunnels are recapped in the table below.

Wind tunnel	S1 MODANE	S2 CHALAISMEUDON
Test section	Circular Diameter 8 m	Circular Diameter 3 m
Max. speed	M = 1	M = .35
Rotor diameter	4 to 5 m	1.5 m
Shaft incidence	- 95° to + 25°	- 24° to + 24°

* Presented at the 7th European Rotorcraft and Powered Lift Aircraft Forum, GARMISCH, September 81.

Fig. 1 gives a general view of the Modane Wind tunnel.

The hubs used are conventional in design. They are articulated in flap pitch and drag with visco-elastic frequency adaptors, with the exception of that of the tilt rotor which only has a pitch articulation.

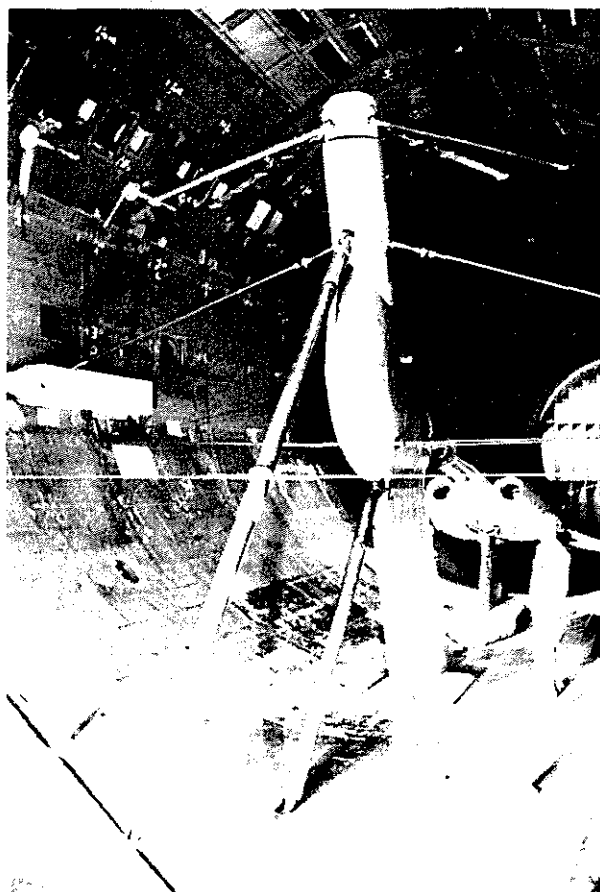


Fig. 1 : S1 MODANE WIND TUNNEL

The hubs of the rotors at Modane have a swash-plate actuated by 3 electro-hydraulic actuators. (Fig. 2).

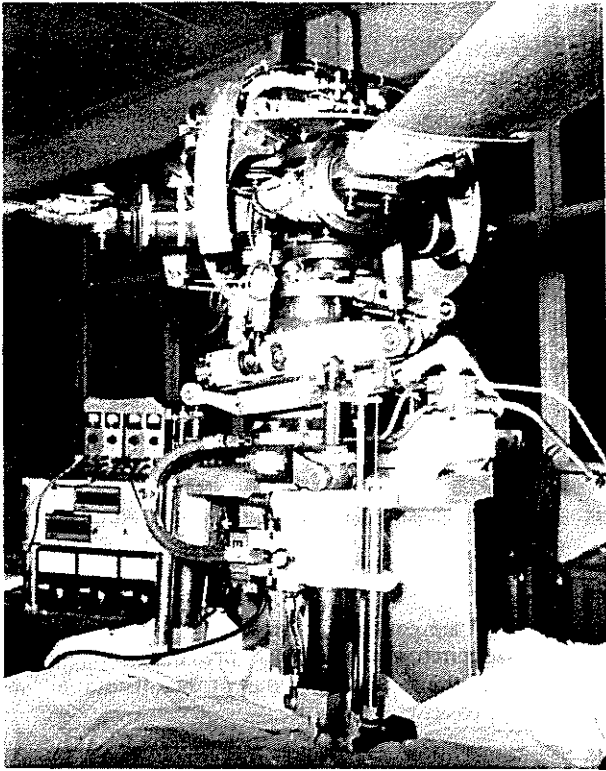


Fig. 2 : ROTOR HUB AND SWASHPLATE (MODANE)

Rotors at Chalais have no swash-plate and the collective pitch can be set when the rotor is stopped.

The testing envelope varies considerably with the hub used (see Fig. 3).

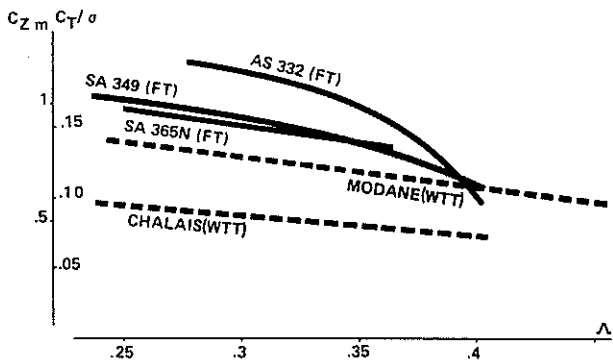


Fig. 3 : AEROSPATIALE ROTORS : WIND TUNNEL AND FLIGHT TEST ENVELOPES

In comparison to actual flight conditions the Reynolds number of Modane rotors is divided by 3 approximately and by 10 for Chalais rotors. This leads to a premature stall of wind-tunnel rotors leading, in turn, to stresses in blades and hub that restrict the testing envelope.

Moreover, maximum lift values are obtained in stabilised configurations during wind-tunnel testing whereas they are obtained during manoeuvres in actual flight (pull out or

bank). Therefore wind-tunnel results for high lifts must be interpreted and corrections must be made through full-scale extrapolation.

The test facilities are now fully operational and wind tunnel test programmes may begin between three and six months after the decision to go ahead has been made in the case of Chalais.

The aim of reducing test costs, compared with those on other available facilities, has been achieved. A test campaign conducted in the S1MA Modane wind tunnel is six to eight times more expensive than one conducted in Chalais. However, it must be pointed out that much more data can be collected at Modane because of the provision for cyclic and collective pitch control from the test room. This also means that it is possible to reach higher rotor propulsive force values. Moreover, it is easier to fit gauges onto the 4 m rotor at Modane than onto our 1.5 m model.

Rather than competing with each other, the two wind tunnel rotor test facilities at Modane and Chalais are complementary : the small scale model may be used to investigate trends quickly and economically, whereas more detailed tests may be conducted in a wider test envelope at Modane.

TILT-ROTOR

A full-scale tilt rotor was tested in the S1 wind tunnel at Modane, reference 1.

This 5 m diameter rotor included 3 tapered blades (500 to 250 mm taper) with non linear twist and thickness-tapered profiles spanwise.

The hub included one pitch hinge only. A swash-plate was used to determine the collective pitch as well as the longitudinal and lateral cyclic pitches.

These tests were carried out to investigate the behaviour of a full scale rotor in every flight configuration : hover, rotary-wing mode, fixed-wing mode, conversion from helicopter to airplane configuration.

In hover (see Fig. 4), performance is determined from tests carried out in a horizontal plane, speed is induced by the rotor on to the section under test. The following results :

$$FM = .72$$

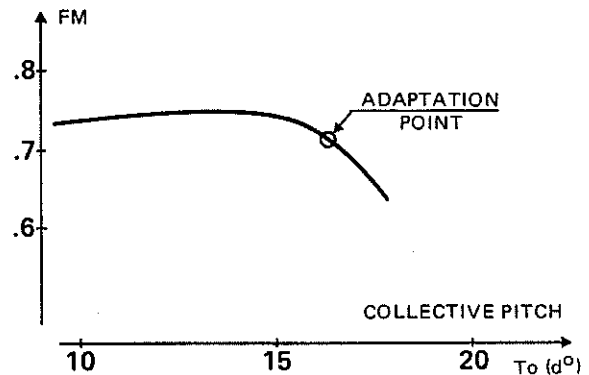


Fig. 4 : TILT ROTOR : FIGURE OF MERIT IN HOVER

were obtained at nominal operating conditions.

Performance tests in cruise flight were carried out up till maximum speed specified for project X 910.

At nominal power, the rotor efficiency varies from 0.89 (100 m/s) to 0.83 (145 m/s) (see Fig. 5).

Complete step-by-step and continuous conversions were carried out without major problems.

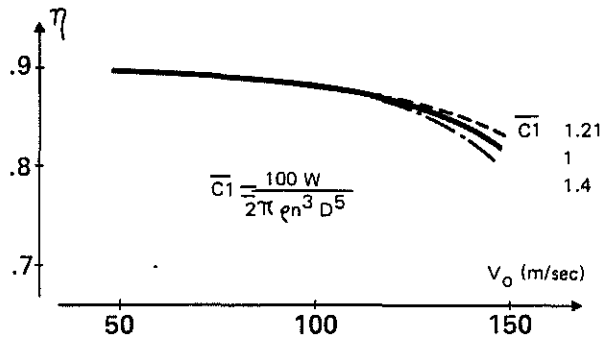


Fig. 5 : TILT ROTOR : CRUISE EFFICIENCY

Piloting rules (see Fig. 6) evolved from step-by-step tilting tests were processed in a computer and slaved to wind tunnel speed.

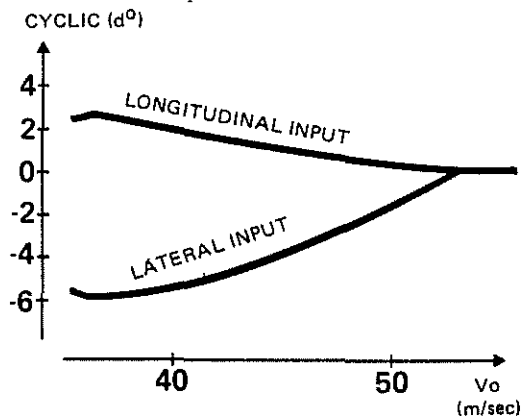
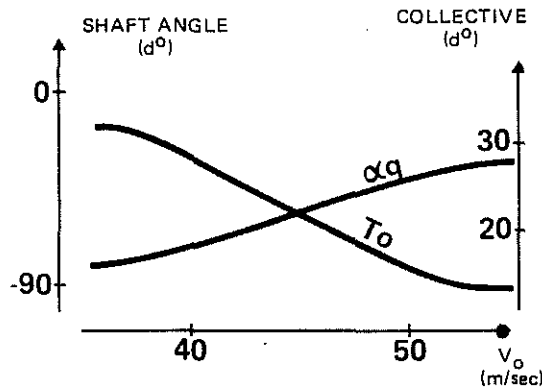


Fig. 6 : PILOTING RULES

Fig. 7 presents some tilt operation results. Variations between continuous and step-by-step tilts are low except for pitch and roll moments.

These differences are thought to spring from Coriolis efforts developed during the fastest conversions (8.3 seconds).

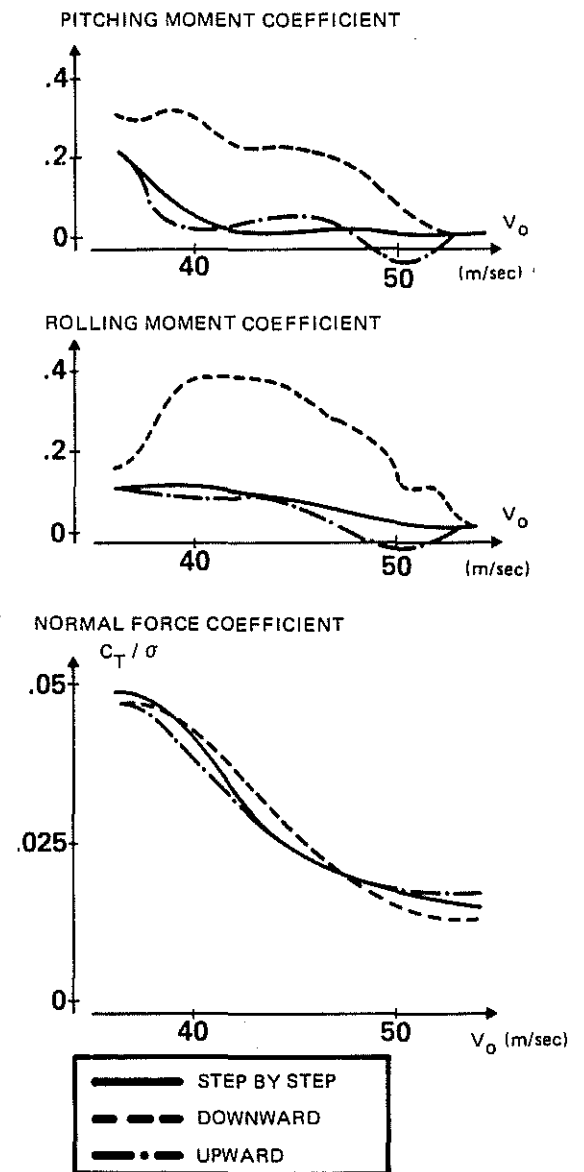


Fig. 7 : TILT OPERATION RESULTS

DEFINITION OF THE ROTORS AT MODANE

With the exception of the rotor of the tilt rotor aircraft, (described under ref. 1) the technology used for the fabrication of blades (see Fig. 8) is very close to that of full-scale rotor composite blades. The spar is made of glass-fiber rovings and the rear part is made of a honeycomb filler.

The skin of the blades is constituted by carbon fiber layers placed at an angle of 45° and whose thickness decreases towards the trailing edge which is fitted with a carbon ledge. Chordwise balancing of the blade is achieved through adding an INERMET counterweight embedded into the spar.

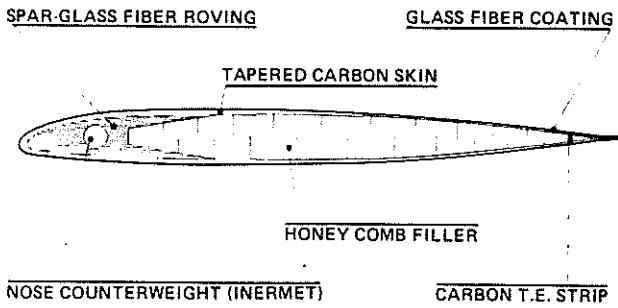


Fig. 8 : MODEL BLADE TECHNOLOGY

From a strictly dynamic point of view the blades of these rotors are not identical with those of full-scale rotor blades yet their torsion frequency is similar with that of the rotors presently used on aircraft.

This point is of particular interest for the study of stall flutter.

The characteristics of the rotors tested are recapped in the table of Fig. 9.

ROTOR REFERENCE	5	6A	6B	7A	7B
(2R)	NACA 0012	OA 209	OA 209	(2R) OA 213	OA 213
(7R)	NACA 0012			(75R) OA 213	OA 213
(85R)	13109-1.58		OA 209	(9R) OA 209	OA 209
(R)	13106-7	OA 209	OA 207	(R) OA 209	OA 206

DIAMETER 4.20 m CHORD .14 m AERODYNAMIC TWIST - 8.3°

Fig. 9 : FOUR-BLADE MODANE ROTORS

HIGH SPEEDS

The range of high speeds was studied in depth during the 4th testing campaign as reported under reference 2.

Fig. 10 shows the general behaviour of the rotor as a function of the rotor disk angle of attack.

The following can be noted

- a high traction area with a forward tilt of the disk which is that of conventional helicopters flying between 0 and 350 km/hr.
- a zero traction or slightly negative traction area where the disk is tilted rearward. In this area the lift is good, the vibration level optimal, the generalised lift-to-drag

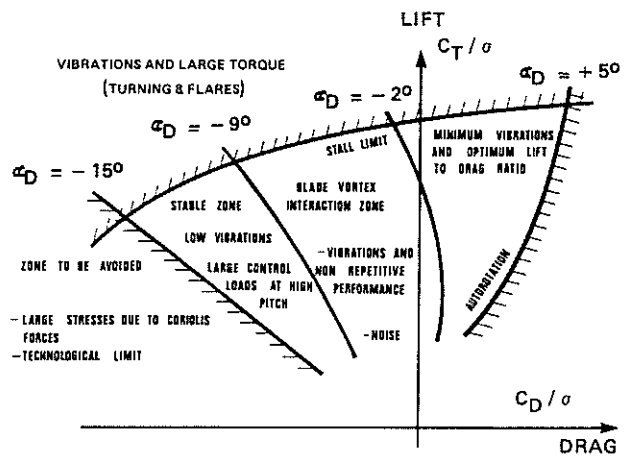


Fig. 10 : GENERAL OPERATING CONDITIONS OF WIND TUNNEL ROTORS

ratio maximal (see Fig. 11). The rotor has a maximum lift-to-drag ratio when it operates close to autorotation and with acceptable lift coefficients ($C_T/\sigma = .068$).

We have shown the existence of a pair of privileged values - lift - lift/drag - throughout the high-speed range.

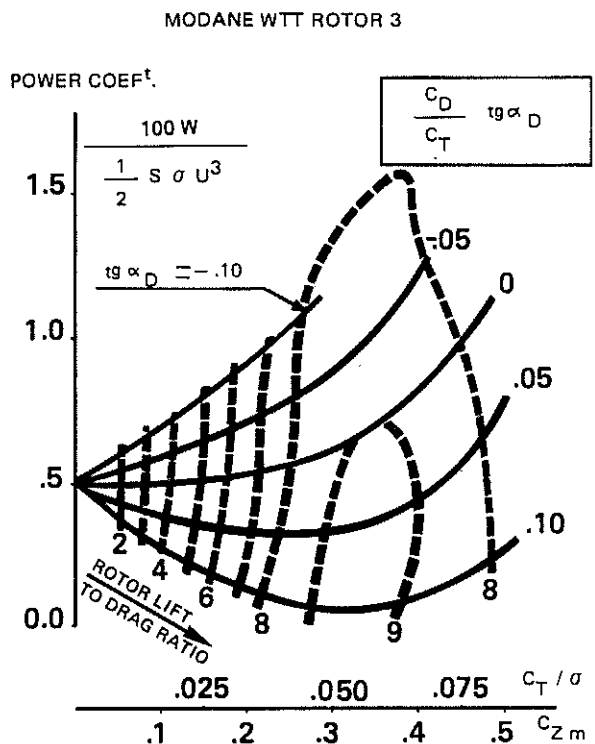


Fig. 11 : ROTOR PERFORMANCE AT HIGH SPEED (414 km/hr)

One of the main lessons we draw from the test is the fact that the lift/drag polar of the rotor becomes independent of the speed and tends to merge with the autorotation polar (see Fig. 12). As a result with a constant lift, the rotor drag is constant.

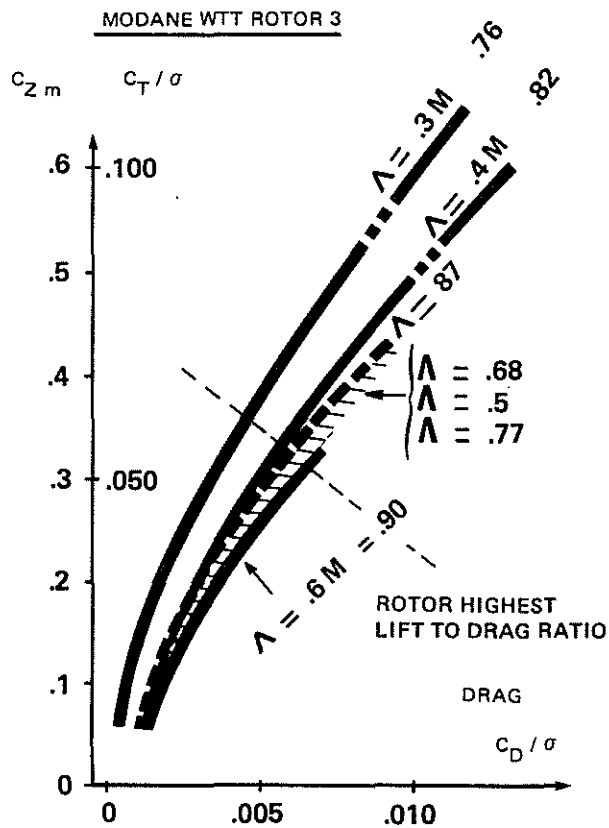


Fig. 12 : ROTOR LIFT-TO-DRAG CHARACTERISTICS (VERTICAL SHAFT)

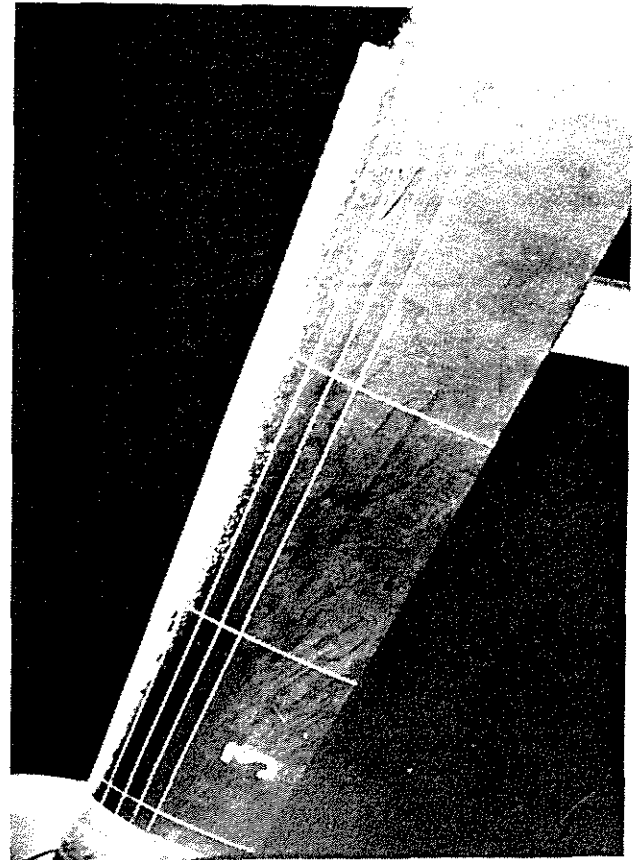


Fig. 13 : ACCRETION ON A MODANE ROTOR BLADE IN ICING CONDITIONS

ICING

The feasibility of icing tests on rotors was demonstrated at S1 wind tunnel at Modane during the winter of 1973-1974 (ref. 3). This installation is particular in that the cold is of natural origin.

A spray grid located before the rotor is used to produce an icing cloud, which makes it possible to study the effects of ice build-up on rotors with a diameter on the order of 4 m.

A theoretical study had previously evidenced the representativeness of artificial icing generated on a mock-up, as regards drop trajectory, ice build-up and shear stresses resulting from centrifugal forces.

New icing tests were carried out in the winter of 1980-1981. The photograph on Fig. 13 shows the ice build-up spanwise on rotor 5. It can be clearly seen, from this shot, that the ice broke due to the centrifugal loads exerted.

Moulds of the ice deposits were taken and they will be compared with those obtained in 2-D flow, Fig. 14

Hardly any refreeze was observed during these tests.

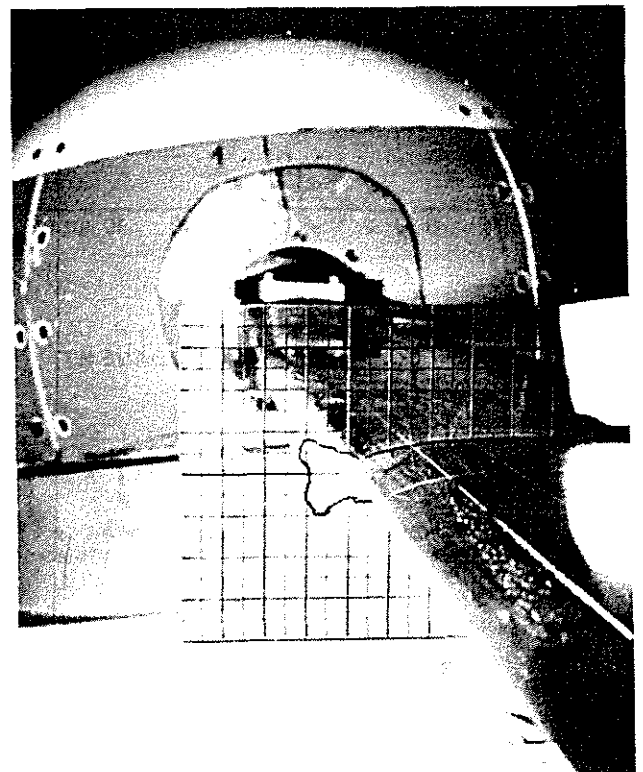


Fig. 14 : SIDE VIEW OF ICE ACCRETION

Icing of the rotor is particularly penalizing. This is verified in fig. 15 by :

- an increase in power demand of + 38 %
- a reduction in rotor traction, at constant pitch, of - 33 %
- a reduction in rotor lift, at constant pitch, of - 8 %.

These tests clearly show it is dangerous to fly in icing conditions with a non-protected rotor.

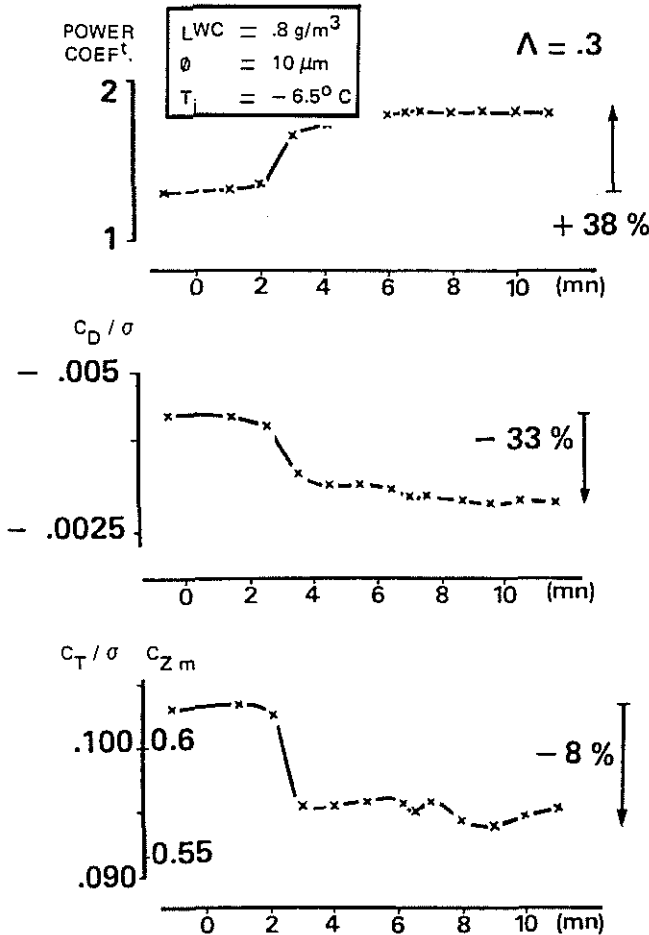


Fig. 15 : ROTOR ICING TESTS (MODANE WT)

VISUALIZATION

A very large number of observations of the airflow on blades and under the rotor were made at Modane (ref. 5).

During the latest campaign, the study on rotor stall was conducted using boundary layer detectors. These semiconductor sensors, developed by ONERA, use the hot film principle.

One of the 7A and 7B rotor blades was fitted with 6 boundary layer detectors located spanwise over 90 % of the leading edge.

Signal variations can be seen (Fig. 16) for a given position of the sensor. The zones of agitation indicate separations ; these tend to spread as loads increase.

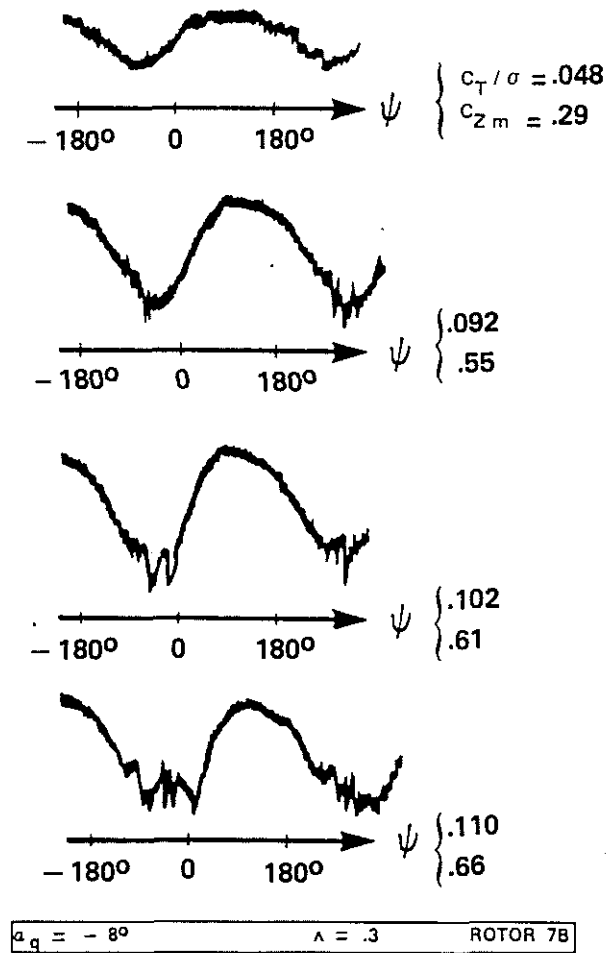


Fig. 16 : BOUNDARY LAYER SIGNAL SENSORS

It has been possible to draw up separation charts (Fig. 17). The separation is focused on the first vortex interference in the retreating blade area.

The separations appearing in the L.H. lower quarter of each figure are due to the hub wake.

VIBRATIONS

Though the dynamic characteristics of the rotors tested at Modane were not exactly similar to that of the rotors installed on aircraft, it was interesting to compare their behaviour as regards vibrations in stall conditions.

Only the total of the 5P and 6P harmonics of the blade torsion signal was taken into consideration since the «stall flutter» phenomenon excites, preferably, those harmonics that are close to the blade torsional frequency (5.2 P) (ref. 4).

Fig. 18 shows the significant gain obtained by using OA airfoils. Between rotors 5 and 6B, taking into consideration realistic operational conditions, the blade torsional response is divided by 2.

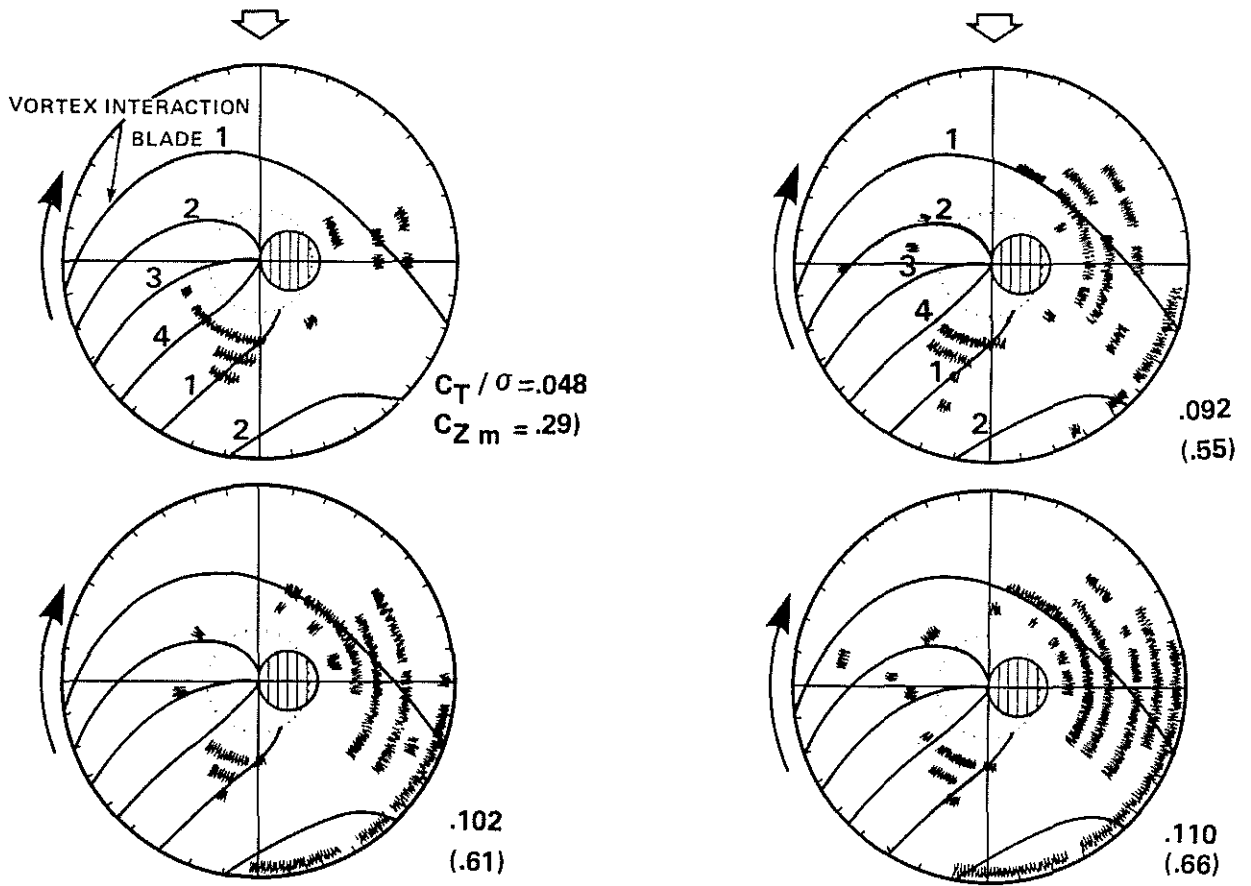


Fig. 17 : SEPARATED FLOW AREAS

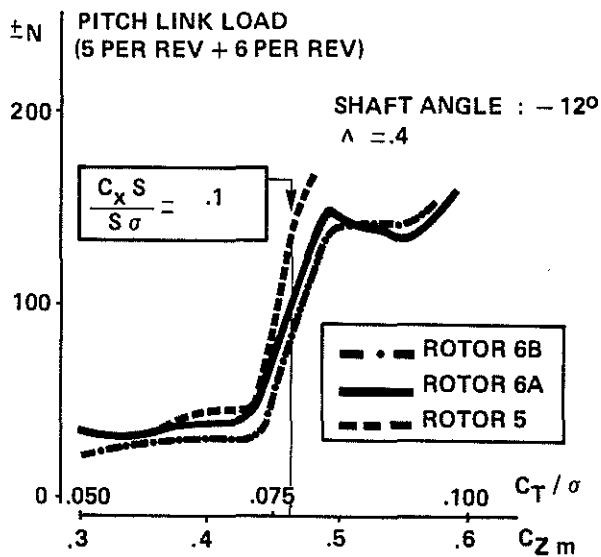


Fig. 18 : BEHAVIOUR OF 5 - 6A - 6B ROTORS IN STALL CONDITIONS

HOVER PERFORMANCE WITH OA AIRFOILS

In quasi-hover rotors 6A and 6B fitted with new generation profiles (OA 209 tapered to OA 207, ref. 6) show an improvement of roughly 3% on rotor figure of merit at nominal thrust, as compared to the reference rotor (rotor 5), fitted with NACA 0012 and NACA modified SA 13109 and SA 13106 sections, Fig. 19 This improvement is mainly due to the higher lift-to-drag ratio of the OA 209 section.

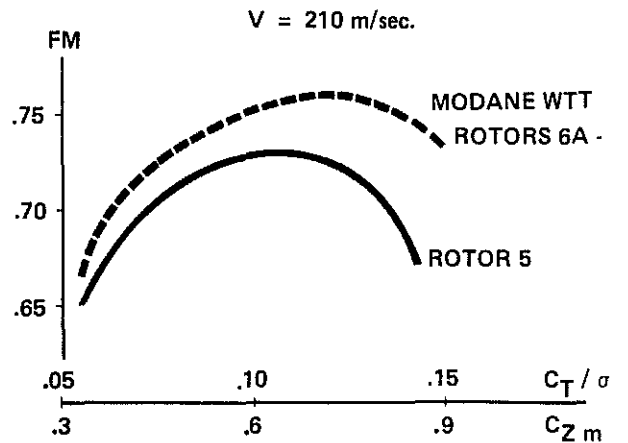


Fig. 19 : EFFECT OF SECTION DISTRIBUTION ON ROTOR PERFORMANCE IN HOVER

It is still more substantial at high loads ($CT/\sigma \geq .11$) as OA airfoils are less sensitive to drag divergence : this appears on Fig. 20 which shows the influence of tip speed on the figure of merit of rotor 6A and 6B as compared to rotor 5. Furthermore, thickness tapering on rotor 6B induces less sensitivity to the compressibility effect for high loads than on rotor 5. These gains were confirmed in flight.

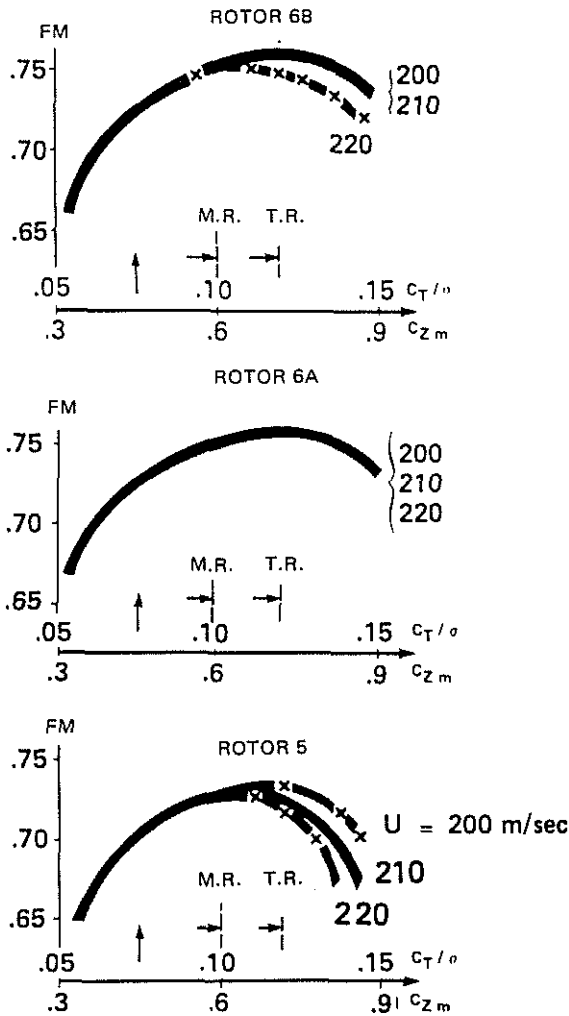


Fig. 20 : COMPRESSIBILITY EFFECT IN HOVER

FORWARD FLIGHT PERFORMANCE WITH OA AIRFOILS

The same rotors are compared in forward flight. Fig. 21 and 22 show the influence of OA family airfoils at high and low propulsive force within the range of medium loads and economical cruise speeds, the gain in performance is negligible. On the contrary, at high loads and speeds, new generation airfoils give a significant improvement.

At very high speed and low propulsive force the tapered end section (OA 207) delays the compressibility effect on the advancing blade, which leads to a very slow evolution of the rotor airfoil power with the advancing blade Mach number : this gives a 4 % improvement in power coefficient at $\Lambda = .45$, nominal thrust.

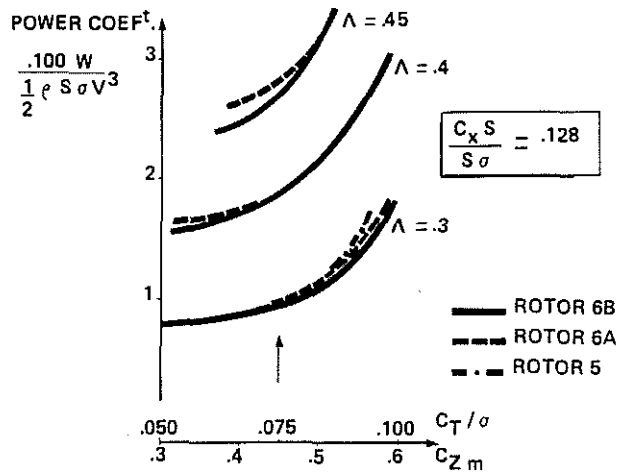


Fig. 21 : LEVEL FLIGHT PERFORMANCE

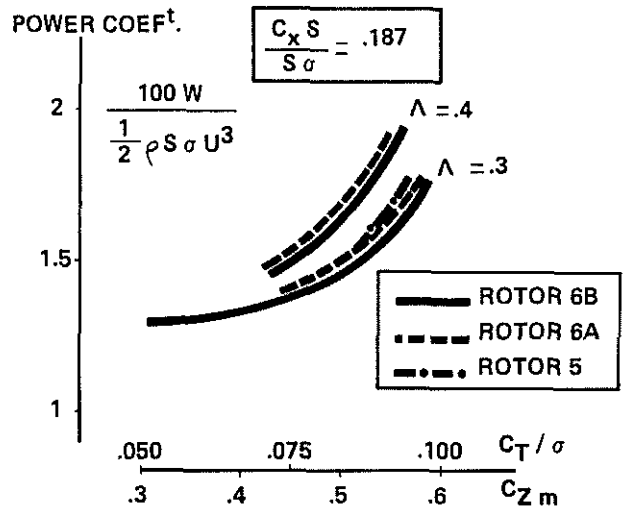


Fig. 22 : LEVEL FLIGHT PERFORMANCE

On Fig. 23 rotors 6B and 7B are compared at a medium propulsive force. On rotor 7B the inboard section of the blade is thickened with the OA 213 airfoil in order to improve the retreating blade stall characteristics. The tip is fitted with an OA 206 which has a higher divergence Mach number than the OA 207 (ref. 7). This definition is favourable whatever the speed at high loads, and at high speed with a good improvement of the power coefficient, up to 9 % at nominal thrust, $\Lambda = .40$ ($V_0 = 300$ km/h).

Theoretical points are plotted. The analysis is based on the conventional momentum theory using 2-D steady airfoil characteristics tested in the 2-D transonic Modane wind tunnel : this program was used to define the section distribution of the various rotors. The theory-to-test correlation is good and could certainly be improved at stall by using full airfoil unsteady characteristics, instead of the present + .12 correction of the CL max. It has not yet been possible to use these characteristics as the 2-D unsteady characteristics of the OA airfoils are not completely known. How-

ver a lot of experiments have been performed already and the analytical formulation is well under way (ref. 8 and 9).

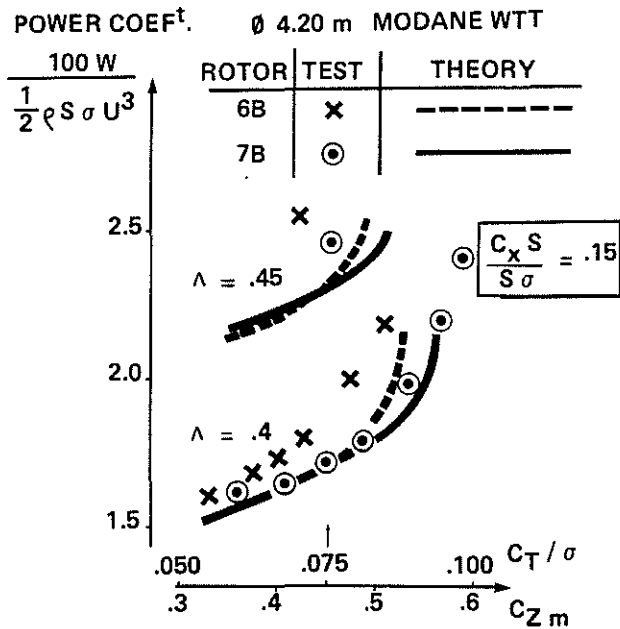


Fig. 23 : EFFECT OF BLADE SECTION DISTRIBUTION ON LEVEL FLIGHT PERFORMANCE

DESCRIPTION OF THE S2 CHALAIS WIND TUNNEL AND TEST FACILITIES

The ONERA S2 wind tunnel at Chalais-Meudon, is an Eiffel type tunnel with a guided air flow. The air duct is 3 m in diameter and its upper and side panels are removable. These panels were removed for the ground run tests.

The rotor is placed in the middle of the air flow and is driven by a hydraulic motor. Discrete values ($-24^\circ \leq \alpha_Q \leq 24^\circ$) are used to set the rotor shaft tilt when the rotor is stopped. Fig. 24 shows the rotor in the air duct.

Total loads on the blades were measured by means of a six-component balance and a torquemeter. A rotating switch was used to transmit blade stress signals.

During the test, the operator had the following monitoring equipment at his disposal :

- Display on two 8-channel oscilloscopes of blade stress bridges and balance dynamometer analogue signals.
- Display on an alpha-numerical console, peripheral of the local T2000/20 computer, of test parameters (V, U, Λ) and aerodynamic loads ($C_T/\sigma, C_D/\sigma, C_Q/\sigma$) corrected by rotor head effects.
- Closed circuit television network to monitor the model in the air flow.

The blade stress bridge and balance dynamometer analogue signals were recorded on magnetic tape and batch processed.

The detailed rotor head and blade development is described under ref. 10. The actual four-blade rotor head is fitted with needle bearing hinges (flapping and drag modes). Collective

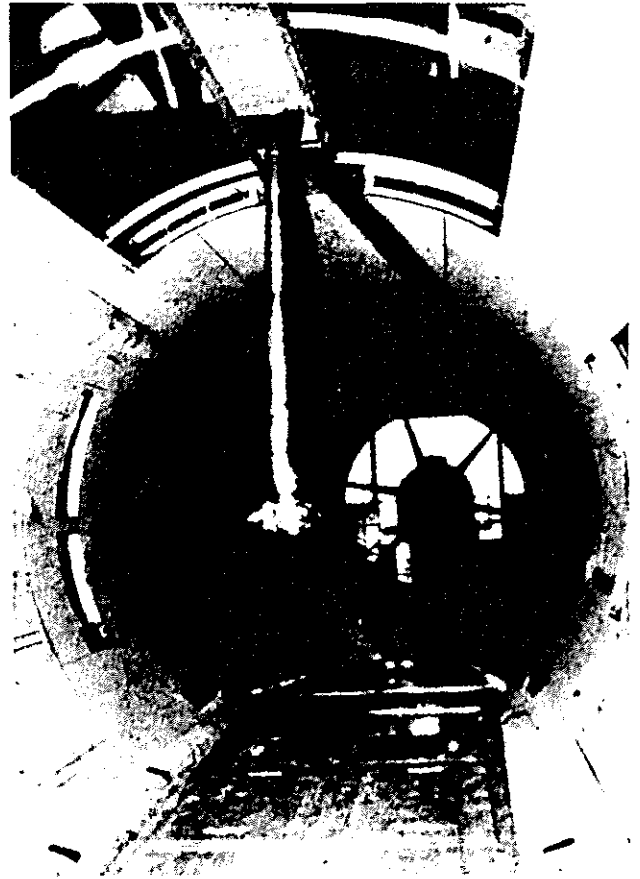


Fig. 24 : S-2 CHALAIS WIND TUNNEL

pitch is set manually when the rotor is stopped, using a clinometer (Fig. 25). Lag frequency adaptors are of the visco-elastic type and are used to prevent ground resonance. A -3° pre-drag angle is set in order to reduce static moments in the blades.

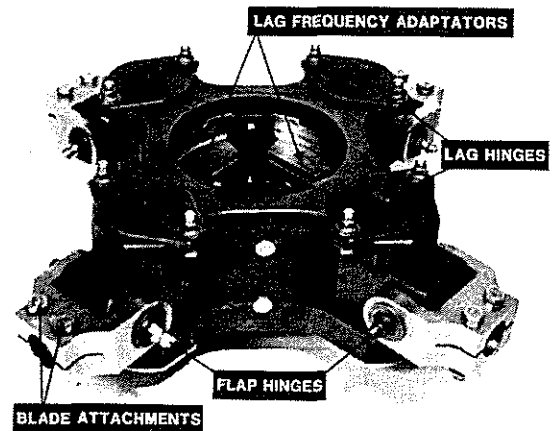


Fig. 25 : CHALAIS FOUR-BLADE ROTOR HUB

Fig.26 shows the blade assembly : in the actual technology the spars are made of fiberglass cloth and the skin of the blade consists of two plies of high tensile strength carbon crossed at 45° angle in order to match the requirements in torsional stiffness, with a first natural torsion frequency

between 5P and 6P.

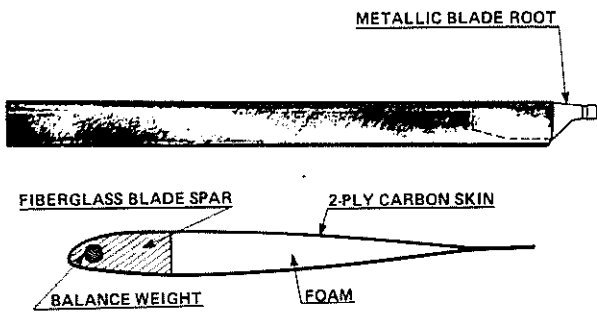


Fig. 26 : CHALAIS MODEL BLADE TECHNOLOGY

Fig. 27 gives a general description of the AEROSPATIALE rotors tested in Chalais with a view to studying the influence of linear and non linear twist and the influence of tip planform on rotor performance and vibratory level. From rotor n° 3 which is taken as a reference rotor, the profile distribution remains invariable with a constant OA 209 airfoil.

4. BLADE ROTOR DIAMETER : 1.474 m CHORD : .05 m

ROTOR MODEL	TWIST	PLANFORM	- PROFILE
1	- 8°	[Diagram of rectangular planform]	BV 23010 1.58
2	- 14°	[Diagram of rectangular planform]	BV 23010 1.58
3 7	- 8° .3 NON LINEAR	[Diagram of rectangular planform]	OA 209
4	- 8° .3	[Diagram of tapered planform]	OA 209
5	- 8° .3	[Diagram of tapered planform]	OA 209
6	- 8° .3	[Diagram of tapered planform]	OA 209

95 R

Fig. 27 : DEFINITION OF AEROSPATIALE ROTORS TESTED IN CHALAIS

The first results were obtained on the two rotors fitted with a BV 23010-1.58 airfoil (- 3° nose down tab) and differing in twist. These results are described under ref. 10. - 8° and - 14° aerodynamic twist could have been compared from the performance and vibratory level point of view. The main conclusions were that in both hover and forward flight, the effect of blade twist on rotor performance is to delay the onset and attenuate the consequences of compressibility effects.

In hover flight, a larger twist angle provides power gains with high disc loads and is therefore particularly advantageous on the main rotor of a crane-helicopter, and especially on a tail rotor.

Flight tests have since been performed and a good qualitative correspondance can be seen between the two sets of results.

In forward flight, the blade twist angle affects the helicopter performance only slightly throughout the standard flight envelope. It is only when high propulsive-force values are to be maintained that it becomes critical.

No significant effect of blade twist on the flapping stresses was recorded at the blade root. However, torsion stresses were increased considerably on a blade with a larger twist angle : stress values at 1 P were twice as large on the rotor with a - 14° twist angle as on the one with a - 8° twist angle. This could be unpractical on an aircraft since an increase in pitch control loads may reduce the service life of control linkage components and may well necessitate the installation of a double control system on light aircraft.

LASER VELOCITY MEASUREMENTS

Experiments were carried out in order to measure the velocity field induced by a four-blade rotor in hover. The purpose of the experiments was an accurate measure of the vertical and tangential velocity components at two vertical coordinates and several azimuthal and radial positions.

Measurements were obtained by means of a two-component laser Doppler velocimeter, developed at ONERA. It uses the conventional technique of interference fringes. It is equipped with Bragg cells which make possible the knowledge of the sign of the velocity. For example, Fig. 28 shows the azimuthal evolutions of the vertical component of the velocity which allow to define precisely the location of the blade tip vortex. Outside of the tip vortex path, velocity varies little with azimuth. All the results were obtained by averaging instantaneous velocities for the four blades (all of them assumed to be identical).

In any case the measurements taken are used by AEROSPATIALE to improve the free wake lifting line hover analysis (ref. 11). Future experiments are planned so as to go further into the knowledge of the rotor wake and its modelization for performance calculations. This code has been used to optimize non-linear twist distribution.

FREE WAKE ANALYSIS AND NON-LINEAR TWIST

In the first version of the hover analysis code the wake was prescribed and was calculated using the modelling formula-

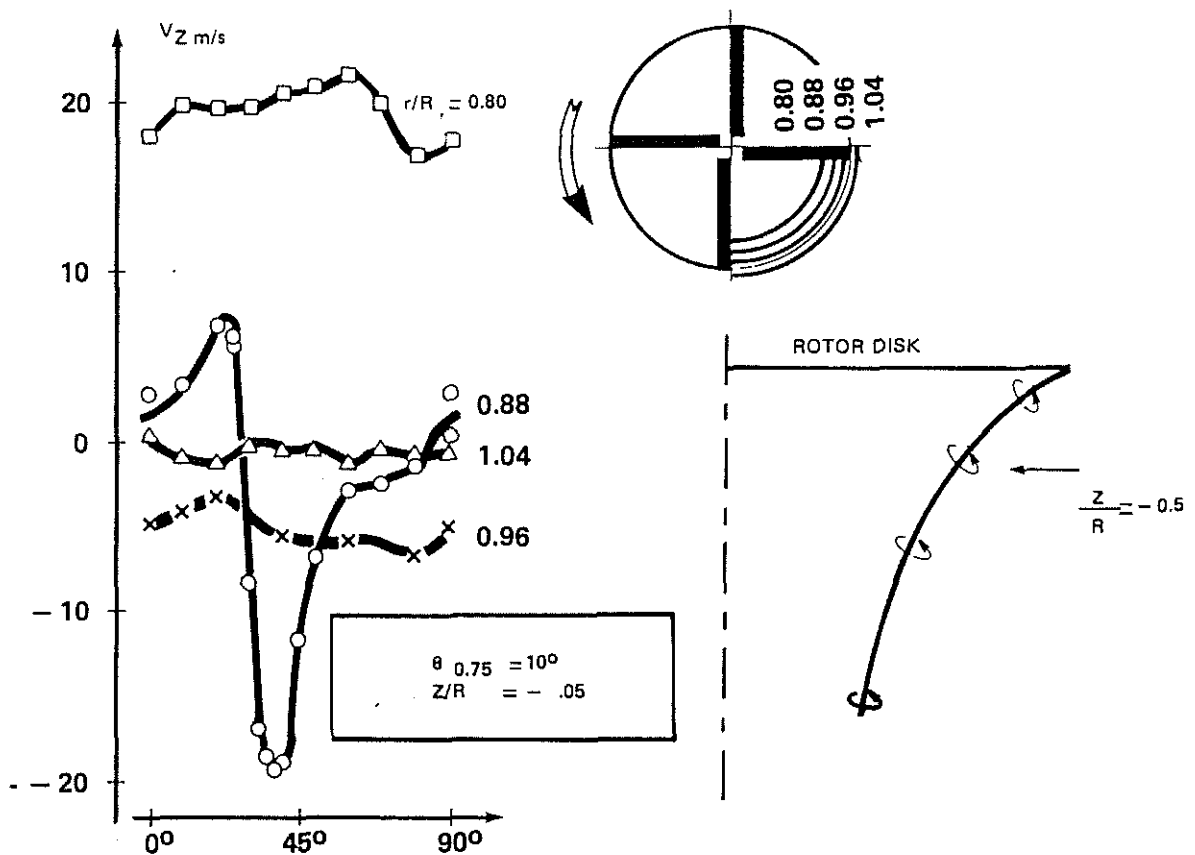


Fig. 28 : VERTICAL COMPONENT VARIATIONS MEASURED BY L.V. IN HOVER

tion given under ref. 12 and 13. In particular the description of the recirculation mechanism proposed under ref. 12 was adopted with a vortex ring located at the fourth passage of the tip vortex beneath a blade and with an intensity four times that of the tip vortex. The applicability of the prescribed schematized wake is relatively limited (i.e. linear twist moderate rotor load, ...) and therefore AEROSPATIALE started research into free wake analysis.

We observed that the effects of the vortex sheets are small when compared to those of the tip vortices and decided to relax only the tip vortex.

The tip vortex has a great effect on the blade itself at the blade tip ($r/R \geq .9$). The influence of the first vortex interaction from the preceding blade is very important since it creates an upwash at the blade tip and a downwash at the inboard portion of the blade (Fig. 29). Non linear twist distribution was obtained by operating the program iteratively in order to minimize mainly the negative effect of this interaction and smooth the incidence distribution on the whole blade. The purpose was to delay rotor stalling. Chalais tests are reported on the same figure and show that this approach was successful. Furthermore the computation gives very good trends: the maximum figure of merit improvement computed was .045 and tests gave .036. The improvement in C_T/σ at maximum figure of merit predicted was .020 which is exactly the test value.

BLADE TIP EXPERIMENTS

Numerous blade tip planforms have been investigated for many years by several helicopter manufacturers or research centers and even tested either in wind tunnels or in flight. Only a few new aircraft are fitted with non-rectangular planforms like for instance swept tips on the UTTAS, tapered tips on the Bell 412, swept tapered tips on the S76 Spirit or on the Aerospatiale Dauphin SA 365 N and Super Puma SA 332. Performance gains, as given by manufacturers are not still clearly established and remain hardly verifiable as the dynamic and aerodynamic problems are often mixed.

Moreover, only since recent developments, in particular on the non-lifting problem (ref. 14, 15, 16, 17, 18), can theoretical methods predict though not accurately - the flow on blade tips which is very complex and depends largely upon the flight configuration.

In order to go further on blade tip potential gains, tests were conducted in Chalais on simple planforms : swept tapered on rotor 4 ; tapered on rotor 5 and parabolic blade tip on rotor 6 as compared to reference rotor No 3.

Profile distribution was constant, all rotors were fitted with an OA 209 airfoil, -8.3° aerodynamic twist - In all comparisons, the reference area is the rectangular blade area.

In hover, Fig. 30, at medium lift coefficient, there is no measured difference between these rotors, apart from the fact that the swept tapered tip presents a surprising figure of merit loss. Close to stall, or for a very high lift, the parabolic tip brings a slight improvement.

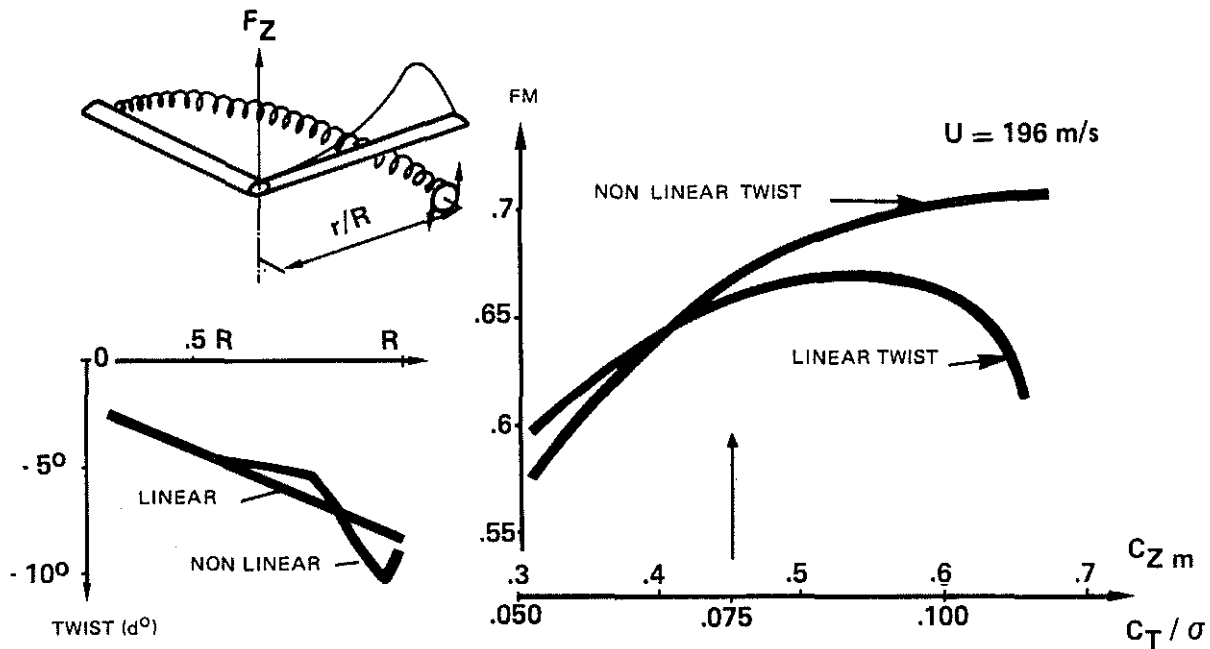


Fig. 29 : INFLUENCE OF BLADE NON LINEAR TWIST ON ROTOR PERFORMANCE

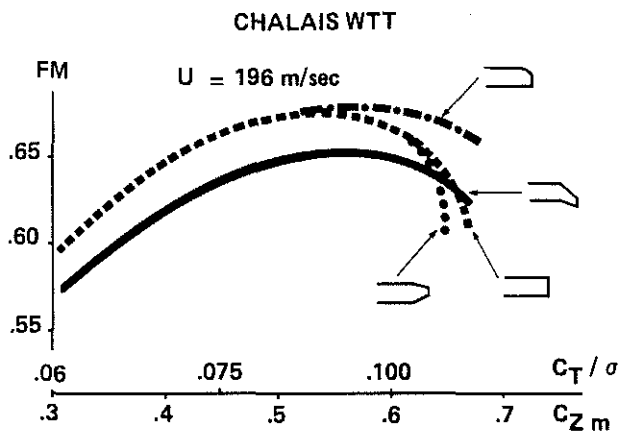


Fig. 30 : EFFECT OF TIP PLANFORM ON ROTOR HOVER PERFORMANCE

The tip speed influence was also tested, as reported on Fig. 31 : at very high load $C_T/\sigma = .105$ close to stall conditions, on the rectangular blade, the figure of merit starts decreasing from $U = 210$ m/sec. up.

On the opposite, the figure of merit of the swept tapered tip remains remarkably unchanged, and overtakes the rectangular blade at $U = 220$ m/sec. which leads to the assumption that there is a compressibility delay effect with that particular shape. The parabolic tip is also slightly favourable.

The overall values of figure of merit and lift coefficient are not really significant because of the scale effect on the Reynolds number which increases the drag coefficient and lowers the CL_{max} . Yet these results are significant from a relative standpoint.

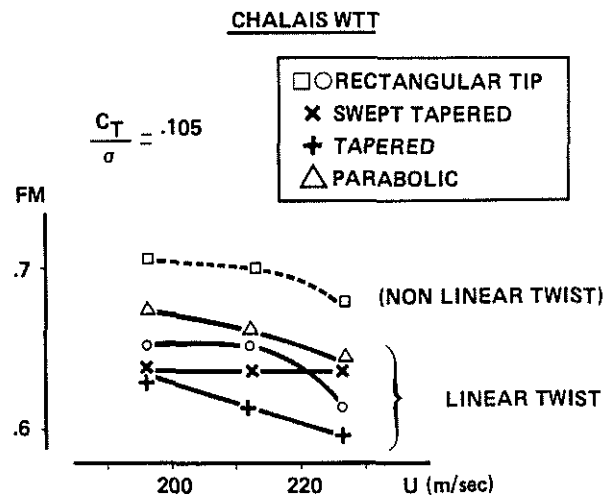


Fig. 31 : TIP SPEED EFFECT IN HOVER FOR VARIOUS BLADE PLANFORM

In forward flight, Fig. 32, level flight performance of various tip shapes could have been compared. The test envelope was described earlier and as regards the detrimental effect of the Reynolds number, it covers a wide range of flight configurations. The main trends at high speed are reported and show that at low and medium propulsive force, the differences between the various rotors are slight and never exceed a 3% range in power coefficient. In this range :

- both the swept tapered and the tapered tips are unfavourable at high loads, and do not bring a noticeable improvement at low lift.
- the parabolic tip is unfavourable at high loads but is

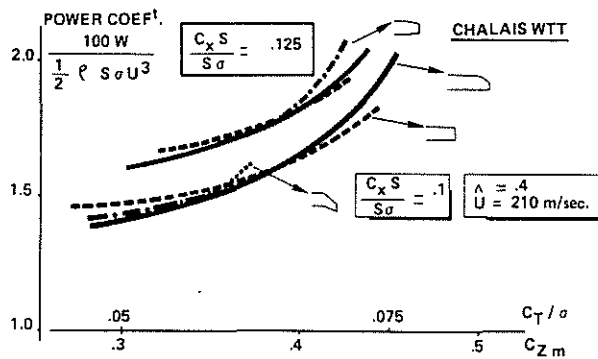


Fig. 32 : LEVEL FLIGHT PERFORMANCE WITH VARIOUS TIP SHAPES

interesting in the case of low loaded rotors - or at nominal lift but at very low speed ($\Lambda \approx .3$). This point is not reported on the figure for the sake of clarity.

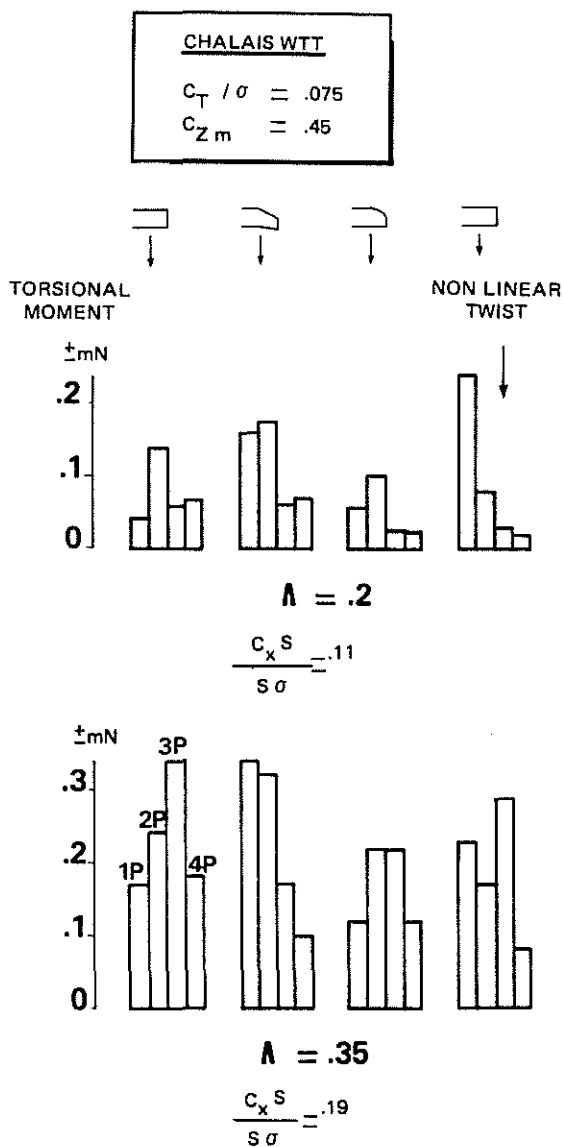


Fig. 33 : BLADE TORSIONAL MOMENT AT ROOT

Non-linear twist, has not been reported either but the major influence is a power loss of 2 % at the most. Comparisons on blade torsional moment at root have been carried out on these tip shapes and show bigger differences, Fig. 33.

- at low speeds, low propulsive force, medium load, swept tapered shape and non-linear twist have a detrimental effect on the 1P component which affects the pitch change rod and the control loads.
- at high speeds, high propulsive force the swept tapered shape shows the biggest 1P component. On the opposite the parabolic shape seems to be better despite a slight difference in the blade torsional characteristics which is not reported on the figure.

SWEPT PARABOLIC TIP SHAPE

Major gains were observed on an ONERA three-blade rotor in Chalais with a swept parabolic tip shape, Fig. 34. In the 250 - 300 km/hr speed range and up to a lift coefficient C_T/σ of .080, the power coefficient improvement is substantial, roughly 7 % at the same lift. This improvement remains practically unchanged whatever the propulsive force. For instance, in the case of a Dauphin SA 365 N, at the same power, this would give an overall improvement of 8 km/hr in maximum speed. This shape is also favourable in hover.

The concept of the swept parabolic shape arose while working on the advancing blade problem and is very promising. With a view to confirming these gains flight tests are planned as well as further analytical and test investigations. These results and the potential developments are discussed in details under ref. 19.

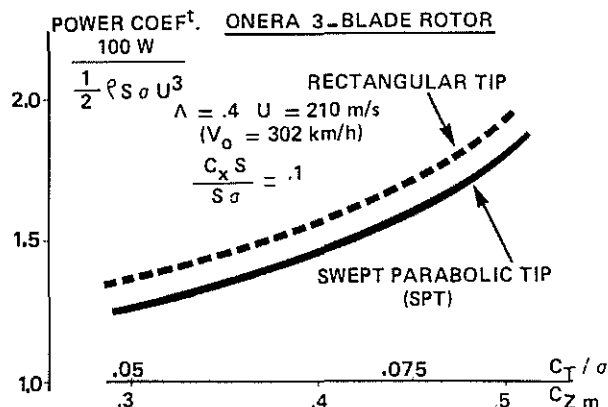


Fig. 34 : PERFORMANCE IMPROVEMENT DUE TO ONERA SPT.

CONCLUSION

Wind tunnel testing allows to estimate with great ease and accuracy the qualities of rotors and to choose those which are worth of flight tests. Such has been the orientation of Aerospatiale for many years already : extensive tests have been conducted in cooperation with ONERA in their Modane and Chalais-Meudon Wind tunnel.

In Modane a complete continuous conversion of a tilt rotor has been performed with success. Very high speeds were reached beyond 500 km/hr with conventional rotors : during autorotation high lift coefficients could be obtained without major drag penalties.

It was possible to determine the effect of icing on a rotor without any de-icing system under conditions that could not have been possible, for safety reasons, during an actual icing-conditions flight.

The airflow on the rotors was measured very accurately (LASER measure, pressures, boundary layer sensors) and the results helped to validate the calculation methods.

Most of the OA family 2-D airfoils characteristic improvements have been checked successfully on Mach scaled rotors with the main following results.

- . good behaviour throughout the entire rotor flight envelope.
- . 3 % improvement on the rotor figure of merit at nominal thrust in hover.
- . 9 % power improvement at nominal thrust and 300 km/hr in level flight.
- . 12 % maximum thrust improvement at stall.

New Aerospatiale helicopters like Dauphin II and Twinstar are fitted with some of these profiles.

Non linear twist and tip planform effects were investigated in Chalais at reduced Reynolds number.

By optimising twist with a view to reducing the negative effects of the vortex interaction, large improvements have been checked in hover at stall.

In level flight, large benefits can be expected with tip planform such as swept parabolic shapes which reduce the local Mach distribution on the advancing blade.

Flight tests are planned which will confirm these results.

REFERENCES

1. M. LECARME Test of a Convertible Aircraft Rotor in the Modane Large Wind Tunnel. Paper No 37. Second European Rotorcraft and Powered Lift Aircraft Forum BUCKEBURG, Sept. 1976.
2. M. LECARME. Comportement d'un rotor au-delà du domaine de vol usuel à la grande Soufflerie de Modane. AGARD -CP 111. MARSEILLE (France) Sept. 1972
3. C. ARMAND, F. CHARPIN, G. FASSO and G. LECCLERE. Techniques and facilities used at the ONERA Modane for icing tests. AGARD-AP-127, Aircraft Icing. OTTAWA (Canada) Sept. 1977.
4. J. GALLOT. Synthèse des problèmes d'aérodynamique instationnaire de l'hélicoptère. AAAF. 15^e. Colloque d'Aérodynamique appliquée. MARSEILLE (France) Nov. 1978.
5. M. LECARME. Airflow over Helicopter Blades. Paper No 18. First European Rotorcraft and Powered Lift Aircraft Forum. SOUTHAMPTON, Sept. 1975.
6. J.J. THIBERT & J. GALLOT. Advanced research on helicopter blade airfoils. Sixth European Rotorcraft and Powered Lift Aircraft Forum. BRISTOL (U.K.) Sept. 1980.
7. J.J. THIBERT & J.M. POURADIER. Design and tests of an helicopter rotor blade with evolutive profile. Twelfth I.C.A.S. Congress. MUNICH (Germany), Oct. 1980.
8. J. RENAUD & J. COULOMB. 2-D Simulation of unsteady phenomena on a rotor. Fourth European Rotorcraft and Powered Lift Aircraft Forum. STRESA (Italy) Sept. 1978.
9. R. DAT, C.T. TRAN & D. PETOT. Phenomenological model of the dynamic stall of a helicopter blade profile. XVI^e Colloque d'Aérodynamique Appliquée (AAAF). LILLE (France), Nov. 1979.
10. A. BREMOND, A. CASSIER & J.M. POURADIER. Design and Wind Tunnel testing of 1.5 m diameter model rotors. Fourth European Rotorcraft and Powered Lift Aircraft Forum. Paper No 13. STRESA (Italy), Sept. 1978.
11. J.M. POURADIER. Aerodynamic study of a hovering rotor. Sixth European Rotorcraft and Powered Lift Aircraft Forum. Paper No 26. BRISTOL (U.K.), Sept. 1980.
12. J.D. KOCUREK & J.L. TANGLER. A prescribed wake lifting surface hover performance analysis. 32nd Annual National Forum of the American Helicopter Society, May 1976.
13. A.J. LANDGREBE. An analytical and experimental investigation of helicopter rotor hover performance and wake geometry characteristics. USAAMRDL TR-71 24, June 1971.
14. M.P. ISOM. Unsteady subsonic and transonic potential flows over helicopter rotor blades, NASA CR-2463, 1974.

15. J.J. CHATTOT. Calculation of three-dimensional unsteady transonic flows past helicopter blades, NASA TP, AVRADCOM TR 80-A-2 (AM), 1980.
16. F.X. CARADONNA, M.P. ISOM. Numerical calculations of unsteady transonic flow over helicopter rotor blades. AIAA Journal, vol. 14 No 4, April 1976.
17. J. GRANT. *The prediction of supercritical pressure distributions on blade tips of arbitrary shape over a range of advancing blade azimuth angles*, 4th European Rotorcraft and Powered Lift Aircraft Forum. STRESA (Italia) Sept. 1978.
18. R. ARIELLI, M.E. TAUBER. *Computation of subsonic and transonic flow about lifting rotor blades*. AIAA Paper No 79-1667. Atmospheric Flight Mechanics Conference, August 1979.
19. J.J. PHILIPPE and J.J. CHATTOT. *Experimental and theoretical studies on helicopter blade tips*. Sixth European Rotorcraft and Powered Lift Aircraft Forum. Paper No 46. BRISTOL (U.K.), Sept. 1980.